Disproof of Bell's Theorem

Illuminating the Illusion of Entanglement

Second Edition

Joy Christian

BrownWalker Press
Boca Raton

by the rotationally non-invariant quantum states such as the GHZ states and the Hardy state—and in fact those predicted by ALL quantum states—can be reproduced exactly in a purely classical, local-realistic manner [7][8][19]. Thus, contrary to the widespread belief, the correlations exhibited by such states are not irreducible quantum effects, but purely local-realistic, topological effects [3][6][8]. Needless to say, this vindicates Einstein's suspicion that quantum state merely describes statistical ensemble of physical systems, and not the individual physical system. It is this inevitable conclusion that Weatherall is resisting.

A.3.3 Another Explicit Simulation of the Model

As mentioned in the caption under Fig. 9.4, Michel Fodje has built another explicit, event-by-event simulation of the model discussed above that is worth elaborating on. While the simulation by Chantal Roth is based on the joint probability density function $|\mathcal{C}(\mathbf{a}, \mathbf{b}; \mathbf{e}_o)|$ defined in (A.9.27), the simulation by Michel Fodje is based on the individual probability density functions $|\mathcal{C}(\mathbf{a}; \mathbf{e}_o)|$ and $|\mathcal{C}(\mathbf{b}; \mathbf{e}_o)|$. We saw in footnote 1 on pages 242 and 243 that the individual probability density functions $p(\mathbf{a}; \mathbf{e}_o, \lambda) = |\cos(\eta_{\mathbf{a}\lambda\mathbf{e}_o})|$ satisfy the relation

$$\frac{1}{4\pi}\int_{S^2} |\cos(\eta_{\mathbf{a}\lambda\mathbf{e}_o})|\ d\Omega \ = \ \frac{1}{2}\sin^2(\eta_{\mathbf{ae}_o})\Big|_0^{\frac{\pi}{2}} \ = \ \frac{1}{2} \qquad \text{(A.9.45)}$$

with respect to any fixed vector $\mathbf{a}$. This suggests that the constraints

$$|\cos(\eta_{\mathbf{ae}_o})| \ \geq \ \frac{1}{2}\sin^2(\theta_o) \ \leq \ |\cos(\eta_{\mathbf{be}_o})| \qquad \text{(A.9.46)}$$

for arbitrary angles $\eta_{\mathbf{ae}_o} \in [0, 2\pi)$ and $\eta_{\mathbf{be}_o} \in [0, 2\pi)$ should play a crucial role in dictating the strength of the correlation between the results $\mathscr{A}(\mathbf{a}; \mathbf{e}_o, \theta_o)$ and $\mathscr{B}(\mathbf{b}; \mathbf{e}_o, \theta_o)$ for a given angle $\theta_o \in [0, \pi/2]$. According to this constraint the probability densities $|\cos(\eta_{\mathbf{ae}_o})|$ and $|\cos(\eta_{\mathbf{be}_o})|$ for observing the measurement results $\mathscr{A}(\mathbf{a}; \mathbf{e}_o, \theta_o)$ and $\mathscr{B}(\mathbf{b}; \mathbf{e}_o, \theta_o)$ depend on the common angle θ_o, just as they depend on the common vector $\mathbf{e}_o$ [9]. This in turn suggests that we may treat $\theta_o \in [0, \pi/2]$ as an additional random parameter, and take the set

$$\Lambda \ := \ \left\{(\mathbf{e}_o, \theta_o) \ \middle| \ |\cos(\eta_{\mathbf{xe}_o})| \ \geq \ \frac{1}{2}\sin^2(\theta_o) \ \ \forall\, \mathbf{x} \in \mathbb{R}^3\right\} \qquad \text{(A.9.47)}$$

as a set of initial or complete states of our physical system [9]. Given one such state, the outcomes of measurements are deterministically determined by the topological constraints within the 3-sphere. From

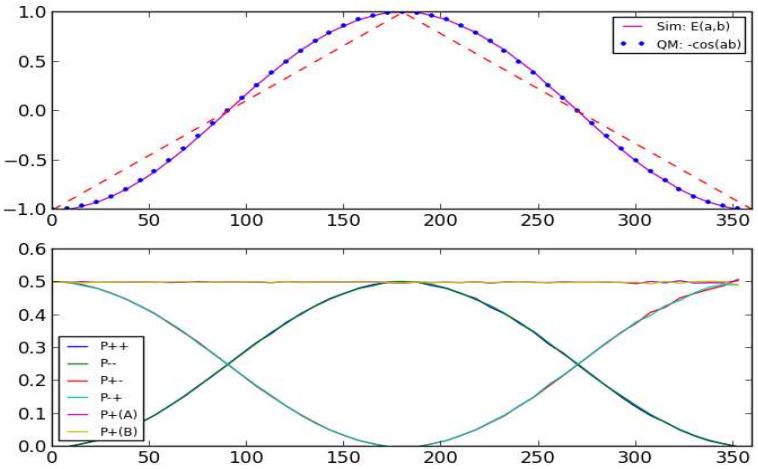

Figure 9.7: Another explicit simulation of the correlation between simultaneously occurring measurement events $\mathscr{A} = \pm 1$ and $\mathscr{B} = \pm 1$ within a parallelized 3-sphere. The code for this simulation is written by Michel Fodje, in Python. Along with other relevant information, it can be downloaded from https://github.com/minkwe/epr-simple/.

a geometrical point of view, the parameter θ_o links two disconnected "sections" of S^3 (*i.e.*, two "orthogonal" 2-spheres within S^3) defined by the bivectors $I \cdot \mathbf{a}$ and $I \cdot \mathbf{b}$, by means of the constraints (A.9.46).

With these considerations, we define the measurement functions as

$$\mathscr{A}(\mathbf{a};\, \mathbf{e}_o,\, \theta_o) \;=\; sign\{-\cos(\,\eta_{\mathbf{a}\mathbf{e}_o}\,)\},\quad \text{for a given } \theta_o \in [0,\, \pi/2]\,, \tag{A.9.48}$$

and

$$\mathscr{B}(\mathbf{b};\, \mathbf{e}_o,\, \theta_o) \;=\; sign\{+\cos(\,\eta_{\mathbf{b}\mathbf{e}_o}\,)\},\quad \text{for a given } \theta_o \in [0,\, \pi/2]\,, \tag{A.9.49}$$

where the vectors $\mathbf{a}$ and $\mathbf{b}$ are specific instances of the vector $\mathbf{x}$. For $\theta_o = 0$ this prescription reduces to that of Bell's own local model [9].

Once again let me stress the obvious that these functions define manifestly *local* measurement results. What is more, given the initial state $(\mathbf{e}_o,\, \theta_o)$, the local outcomes $\mathscr{A}(\mathbf{a};\, \mathbf{e}_o,\, \theta_o)$ and $\mathscr{B}(\mathbf{b};\, \mathbf{e}_o,\, \theta_o)$ are deterministically and ontologically determined to be either $+1$ or -1,

for any *freely chosen* vectors $\mathbf{a}$ and $\mathbf{b}$, where $\mathbf{e}_o$ is a random vector on S^2 as defined before, and θ_o is a random angle, chosen from the interval $[0,\, \pi/2]$. The correlation is then calculated quite simply as

$$\mathcal{E}(\mathbf{a},\, \mathbf{b}) \,=\, \lim_{n \gg 1} \left[\frac{1}{n} \sum_{i\,=\,1}^{n} \mathscr{A}(\mathbf{a};\, \mathbf{e}_o^i,\, \theta_o^i)\, \mathscr{B}(\mathbf{b};\, \mathbf{e}_o^i,\, \theta_o^i) \right] \,=\, -\,\mathbf{a}\cdot\mathbf{b}\,. \tag{A.9.50}$$

For the measurement functions defined in (A.9.48) and (A.9.49), the probabilities of observing the specific outcomes $+1$ or -1 turn out to be exactly $1/2$, with 100% detector efficiency. In other words, every particle that emerges in a state $(\mathbf{e}_o,\, \theta_o)$ ends up being detected by the detector, just as in the previous simulation. On the other hand, the probabilities of jointly observing the results $\mathscr{A}(\mathbf{a};\, \mathbf{e}_o,\, \theta_o)$ and $\mathscr{B}(\mathbf{b};\, \mathbf{e}_o,\, \theta_o)$ turn out to be exactly those predicted by quantum mechanics [cf. Eqs. (A.9.37) to (A.9.40)]. Consequently, not only the correlations between the results turn out to be those predicted by quantum mechanics [cf. Eq. (A.9.41)], but also the Clauser-Horne inequality is necessarily violated in this simulation [cf. Eq. (A.9.44)].

It is important to recognize that the strength of the correlation exhibited in this simulation does not stem from exploiting any known or unknown loopholes—such as the detection loophole. Needless to say, a measurement event cannot occur if there does not exist a state that can bring about that event. If there are no clouds in the sky in the first place, then there can be no rain, no matter where one goes. As we noted, the state of the spin system is specified by the pair $(\mathbf{e}_o,\, \theta_o)$ defined by the set (A.9.47)—not just by $\mathbf{e}_o$. In other words, the initial distribution of the physical states is defined by the set

$$\Lambda \,:=\, \left\{ (\mathbf{e}_o,\, \theta_o) \;\middle|\; |\cos(\,\eta_{\mathbf{x}\mathbf{e}_o})| \,\geq\, \frac{1}{2}\,\sin^2(\,\theta_o\,) \quad \forall\, \mathbf{x} \in \mathbb{R}^3 \right\}, \tag{A.9.51}$$

which reduces to that of Bell's local model [9] for $\theta_o = 0 = \textit{constant}$. Accordingly, since there are no states of the physical system for which $|\cos(\,\eta_{\mathbf{x}\mathbf{e}_o})| \,<\, \frac{1}{2}\,\sin^2(\,\theta_o\,)$ holds true for any $\mathbf{x}$, a measurement event cannot possibly occur for $|\cos(\,\eta_{\mathbf{x}\mathbf{e}_o})| \,<\, \frac{1}{2}\,\sin^2(\,\theta_o\,)$, no matter what $\mathbf{x}$ is [9]. If $\mathbf{x}$ happens to be equal to $\mathbf{b}$, for example, then there is no reason for the detector at $\mathbf{b}$ to click when $|\cos(\,\eta_{\mathbf{b}\mathbf{e}_o})| \,<\, \frac{1}{2}\,\sin^2(\,\theta_o\,)$, even for the non-vanishing random angles θ_o in the interval $[0,\, \pi/2]$.

Independently of this physical picture, it is also instructive to view the simulation purely from the perspective of computability. From this perspective the correlation is calculated as follows: Alice freely chooses a vector $\mathbf{a}$ on S^2. She is then given four scalar numbers,

$$(\theta_o,\, e_o^x,\, e_o^y,\, e_o^z)\,, \tag{A.9.52}$$

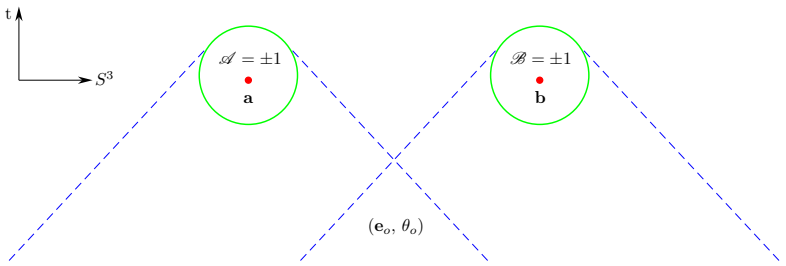

Figure 9.8: The measurement results $\mathscr{A}(\mathbf{a}; \mathbf{e}_o, \theta_o)$ and $\mathscr{B}(\mathbf{b}; \mathbf{e}_o, \theta_o)$ are deterministically brought about by the common cause $(\mathbf{e}_o, \theta_o)$.

or a pair $(\mathbf{e}_o, \theta_o)$, represented by a randomly chosen vector $\mathbf{e}_o$ on S^2 and a randomly chosen scalar θ_o from the interval $[0, \pi/2]$. Similarly, Bob freely chooses a vector $\mathbf{b}$ on S^2, and is also given the same four scalar numbers $(\mathbf{e}_o, \theta_o)$. Using these scalars Alice and Bob compute the numbers $\mathscr{A}(\mathbf{a}; \mathbf{e}_o, \theta_o)$ and $\mathscr{B}(\mathbf{b}; \mathbf{e}_o, \theta_o)$, respectively, as follows:

$$\mathscr{A}(\mathbf{a}; \mathbf{e}_o, \theta_o) = \begin{cases} sign\{-\cos(\eta_{\mathbf{ae}_o})\} & \text{if } |\cos(\eta_{\mathbf{ae}_o})| \geq \frac{1}{2}\sin^2(\theta_o) \\ 0 & \text{if } |\cos(\eta_{\mathbf{ae}_o})| < \frac{1}{2}\sin^2(\theta_o) \end{cases} \tag{A.9.53}$$

and

$$\mathscr{B}(\mathbf{b}; \mathbf{e}_o, \theta_o) = \begin{cases} sign\{+\cos(\eta_{\mathbf{be}_o})\} & \text{if } |\cos(\eta_{\mathbf{be}_o})| \geq \frac{1}{2}\sin^2(\theta_o) \\ 0 & \text{if } |\cos(\eta_{\mathbf{be}_o})| < \frac{1}{2}\sin^2(\theta_o). \end{cases} \tag{A.9.54}$$

This prescription simply partitions the outcomes $\mathscr{A}(\mathbf{a}; \mathbf{e}_o, \theta_o)$ and $\mathscr{B}(\mathbf{b}; \mathbf{e}_o, \theta_o)$ into three sets of numbers, $+1$, -1, and 0, which are then summed over the full ranges of the possible vectors $\mathbf{e}_o$ and possible scalars θ_o, giving the vanishing local averages:

$$\lim_{n \gg 1}\left[\frac{1}{n}\sum_{i=1}^{n}\mathscr{A}(\mathbf{a}; \mathbf{e}_o^i, \theta_o^i)\right] = 0 = \lim_{n \gg 1}\left[\frac{1}{n}\sum_{i=1}^{n}\mathscr{B}(\mathbf{b}; \mathbf{e}_o^i, \theta_o^i)\right], \tag{A.9.55}$$

where n is the total number of non-vanishing outcomes in the sets.

Alice and Bob then multiply the outcomes $\mathscr{A}(\mathbf{a}; \mathbf{e}_o, \theta_o)$ and $\mathscr{B}(\mathbf{b}; \mathbf{e}_o, \theta_o)$ for each pair $(\mathbf{e}_o, \theta_o)$, add all of the products together,

and divide the sum by the total number of non-vanishing products (*i.e.*, "coincidences") they have added. The result is the correlation

$$\mathcal{E}(\mathbf{a},\,\mathbf{b}) \;=\; \lim_{n\gg 1}\left[\frac{1}{n}\sum_{i=1}^{n}\mathscr{A}(\mathbf{a};\,\mathbf{e}_o^i,\,\theta_o^i)\,\mathscr{B}(\mathbf{b};\,\mathbf{e}_o^i,\,\theta_o^i)\right] \;=\; -\,\mathbf{a}\cdot\mathbf{b}\,. \tag{A.9.56}$$

Thus, regardless of the interpretation given to numbers $\mathscr{A}(\mathbf{a};\,\mathbf{e}_o,\,\theta_o)$ and $\mathscr{B}(\mathbf{b};\,\mathbf{e}_o,\,\theta_o)$, we have arrived at a refutation of Bell's theorem[4].

A.3.4 Exploring the World Beyond the Quantum World

It turns out that the simulation discussed above can be generalized to generate correlations of *any* strength—from the weakest possible (Bell's model) to the strongest possible (the box model), provided the distribution of the complete states is generalized from (A.9.51) to

$$\Lambda \;:=\; \left\{(\mathbf{e}_o,\,\theta_o,\,l_o)\;\middle|\;|\cos(\,\eta_{\mathbf{x}\mathbf{e}_o})|\;\geq\;l_o\,\sin^2(\,\theta_o\,)\;\;\forall\,\mathbf{x}\in\mathbb{R}^3\right\}, \tag{A.9.57}$$

with the scalar $l_o \in [0,\,1]$ being an additional, *non-random* common cause [cf. Fig. 9.9]. The two measurement functions are then given by

$$\mathscr{A}(\mathbf{a};\,\mathbf{e}_o,\,\theta_o,\,l_o) \;=\; sign\{-\cos(\,\eta_{\mathbf{a}\mathbf{e}_o}\,)\},\;\;\text{for a given pair}\;\;(\theta_o,\,l_o)\,, \tag{A.9.58}$$

and

$$\mathscr{B}(\mathbf{b};\,\mathbf{e}_o,\,\theta_o,\,l_o) \;=\; sign\{+\cos(\,\eta_{\mathbf{b}\mathbf{e}_o}\,)\},\;\;\text{for a given pair}\;\;(\theta_o,\,l_o)\,, \tag{A.9.59}$$

where the *freely chosen* vectors $\mathbf{a}$ and $\mathbf{b}$ are specific instances of the vector $\mathbf{x}$, just as before. The correlation between the measurement results $\mathscr{A}(\mathbf{a};\,\mathbf{e}_o,\,\theta_o,\,l_o)$ and $\mathscr{B}(\mathbf{b};\,\mathbf{e}_o,\,\theta_o,\,l_o)$ can then be determined as usual by computing the expectation value of their scalar product:

$$\mathcal{E}(\mathbf{a},\,\mathbf{b}) \;=\; \lim_{n\gg 1}\left[\frac{1}{n}\sum_{i=1}^{n}\mathscr{A}(\mathbf{a};\,\mathbf{e}_o^i,\,\theta_o^i,\,l_o^i)\,\mathscr{B}(\mathbf{b};\,\mathbf{e}_o^i,\,\theta_o^i,\,l_o^i)\right]. \tag{A.9.60}$$

[4] The original simulation by Michel Fodje confirming the above results has been translated by John Reed from Python to Mathematica. It can be found in PDF format at this page: http://libertesphilosophica.info/Minkwe_Sim_J_Reed.pdf.

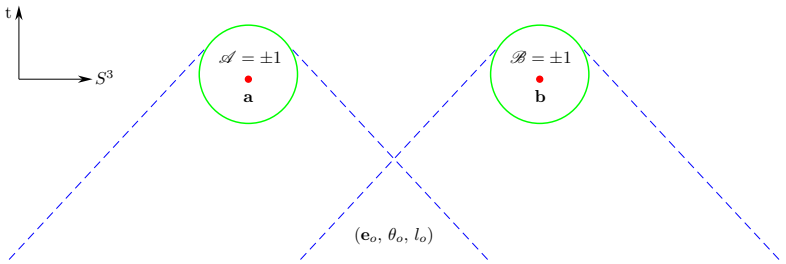

Figure 9.9: The measurement results $\mathscr{A}(\mathbf{a}; \mathbf{e}_o, \theta_o)$ and $\mathscr{B}(\mathbf{b}; \mathbf{e}_o, \theta_o)$ are deterministically brought about by the initial state $(\mathbf{e}_o, \theta_o, l_o)$.

Special Case (1): Weakest Possible Correlation—Bell's Model:

If we now fix either $\theta_o = 0$ or $l_o = 0$ (or both $= 0$) in the distribution (A.9.57), for all $\mathbf{e}_o$, it reduces to that of Bell's own local model [9],

$$\Lambda \;=\; \left\{ (\mathbf{e}_o,\, \theta_o = 0 \text{ or } l_o = 0) \;\middle|\; |\cos(\,\eta_{\mathbf{x}\mathbf{e}_o})| \;\geq\; 0 \quad \forall\, \mathbf{x} \in \mathbb{R}^3 \right\}, \tag{A.9.61}$$

generating the weakest possible (or "classical") correlation:

$$\mathcal{E}(\mathbf{a},\, \mathbf{b}) \;=\; \begin{cases} -1 \;+\; \frac{2}{\pi}\,\eta_{\mathbf{a}\mathbf{b}} & \text{if} \quad 0 \leq \eta_{\mathbf{a}\mathbf{b}} \leq \pi \\ \\ +3 \;-\; \frac{2}{\pi}\,\eta_{\mathbf{a}\mathbf{b}} & \text{if} \quad \pi \leq \eta_{\mathbf{a}\mathbf{b}} \leq 2\pi\,. \end{cases} \tag{A.9.62}$$

Special Case (2): Strongest Possible Correlation—the Box Model:

On the other hand, if we fix $\theta_o = \pi/2$ and $l_o = 1$ in the distribution (A.9.57), again for all $\mathbf{e}_o$, it reduces to that of the "box" model,

$$\Lambda \;=\; \left\{ (\mathbf{e}_o,\, \theta_o = \pi/2,\, l_o = 1) \;\middle|\; |\cos(\,\eta_{\mathbf{x}\mathbf{e}_o})| \;\geq\; 1 \quad \forall\, \mathbf{x} \in \mathbb{R}^3 \right\}, \tag{A.9.63}$$

generating the strongest possible (albeit unphysical) correlation:

$$\mathcal{E}(\mathbf{a},\, \mathbf{b}) \;=\; \begin{cases} -1 \quad \text{if} \quad 0 \leq \eta_{\mathbf{a}\mathbf{b}} < \pi/2 \quad \text{or} \quad 3\pi/2 < \eta_{\mathbf{a}\mathbf{b}} \leq 2\pi \\ \\ +1 \quad \text{if} \quad \pi/2 < \eta_{\mathbf{a}\mathbf{b}} < 3\pi/2\,. \end{cases} \tag{A.9.64}$$

Special Case (3): "Quantum" Correlation—the 3-Sphere Model:

Finally, if we set $l_o = 1/2$ in the distribution (A.9.57), again for all $\mathbf{e}_o$, but keep θ_o random, then we are led back to the distribution

$$\Lambda \,=\, \left\{ \left(\mathbf{e}_o,\, \theta_o,\, l_o = \frac{1}{2} \right) \;\middle|\; |\cos(\,\eta_{\mathbf{x}\mathbf{e}_o})| \,\geq\, \frac{1}{2}\,\sin^2(\,\theta_o\,) \;\;\forall\, \mathbf{x} \in \mathbb{R}^3 \right\}, \tag{A.9.65}$$

generating the "quantum" correlation discussed above. Thus, if we view $l_o = 1/2$ as the average of the extremes $l_o = 0$ and $l_o = 1$, then the key feature that generates precisely the quantum correlation is the randomness of θ_o, channeled through the geometrical constraint

$$|\cos(\,\eta_{\mathbf{x}\mathbf{e}_o})| \,\geq\, \frac{1}{2}\,\sin^2(\,\theta_o\,) \;\;\forall\, \mathbf{x} \in \mathbb{R}^3. \tag{A.9.66}$$

A.3.5 Elegant, Powerful, and Succinct Calculation of the Correlation

The above simulations once again confirm the fact that EPR-Bohm correlations are local-realistic correlations among the binary points of a parallelized 3-sphere [6]. As we saw in section 9.2, however, this fact can be expressed more elegantly by understanding how random errors propagate within a parallelized 3-sphere. In particular, we saw that EPR-Bohm correlations can be derived by recognizing that the raw scores $\mathscr{A}(\mathbf{a},\,\lambda)$ and $\mathscr{B}(\mathbf{b},\,\lambda)$ are generated within S^3 with *different* bivectorial scales of dispersion, and hence the correct correlation between them can be determined only by calculating the covariation of the corresponding standardized variables $\mathbf{L}(\mathbf{a},\,\lambda)$ and $\mathbf{L}(\mathbf{b},\,\lambda)$:

$$\begin{aligned} \mathcal{E}(\mathbf{a},\,\mathbf{b}) \,&=\, \lim_{n \gg 1} \left[\frac{1}{n} \sum_{i\,=\,1}^{n} \mathscr{A}(\mathbf{a},\,\lambda^i)\;\mathscr{B}(\mathbf{b},\,\lambda^i) \right] \\ &=\, \lim_{n \gg 1} \left[\frac{1}{n} \sum_{i\,=\,1}^{n} \mathbf{L}(\mathbf{a},\,\lambda^i)\mathbf{L}(\mathbf{b},\,\lambda^i) \right] \\ &=\, -\,\mathbf{a}\cdot\mathbf{b}\,, \end{aligned} \tag{A.9.67}$$

where

$$\begin{aligned} \mathbf{L}(\mathbf{a},\,\lambda^i)\,\mathbf{L}(\mathbf{b},\,\lambda^i) \,&\equiv\, -\,\mathbf{a}\cdot\mathbf{b} \,-\, \mathbf{L}(\mathbf{a}\times\mathbf{b},\,\lambda^i) \\ &\equiv\, -\,\mathbf{a}\cdot\mathbf{b} \,-\, \lambda^i\,\mathbf{D}(\mathbf{a}\times\mathbf{b}), \end{aligned} \tag{A.9.68}$$

and the standardized variables are defined as

$$\mathbf{L}(\mathbf{a},\,\lambda) \,:=\, \frac{\mathbf{q}(\psi,\,\mathbf{a},\,\lambda) \,-\, m(\mathbf{q})}{\sigma[\,\mathbf{q}(\psi,\,\mathbf{a},\,\lambda)]} \,=\, \frac{\mathscr{A}(\mathbf{a},\,\lambda) \,-\, m(\mathscr{A})}{\sigma[\,\mathscr{A}(\mathbf{a},\,\lambda)]}\,. \tag{A.9.69}$$